Ultrawideband Millimeterwave Robotic Antenna Measurements enabled by FMCW Radar Sensors

Kristof Dausien*, Tobias Körner*, Christian Schulz*, Nils Pohl†, Ilona Rolfes*, Jan Barowski*
*(Affiliation): Institute of Microwave Systems, Ruhr University Bochum, Bochum, Germany, kristof.dausien@rub.de
†(Affiliation): Institute of Integrated Systems, Ruhr University Bochum, Bochum, Germany

***Abstract*—In this paper ultrawideband frequency modulated continuous wave (FMCW) radar sensors in D-band are used to provide a coherent (magnitude and phase) measurement of an antenna pattern. The antenna under test (AUT) is mounted on the radar sensor using a standard waveguide flange. Due to the compactness of the sensor and its integrated signal source, it is easily moveable by a robotic plattform. Only an ethernet connection to a host PC is required, strongly simplifying cable handling on the robot. The coherent pattern measurement is enabled by performing radar echo measurements (in reflection) onto a probe antenna. A switchable load at the probe antenna feed is utilized to improve the dynamic range and to remove undesired environmental reflections by performing a differential measurement.**

***Index Terms*—antenna measurement, electromagnetics, radar, robot, ultrawideband.**

I. Introduction

Robot-enabled antenna measurements are well established nowadays, due to the increasing availability of precise robotic positioning units and improving accessibility of the tool-chain to control these. In addition to the positioning unit, accurate instrumentation for the millimeterwave (mmWave) frequency is needed, as well. Considering the characterization of passive antennas, i.e. without integrated signal sources or detectors, this is usually achieved by either using a vector network analyzer (VNA) [1] or a combination of a signal generator and a signal or spectrum analyzer. Of course, the VNA comes with the advantages that the full S-parameter matrix can be measured (including return loss) and that it provides phase accurate transmission parameters. Thus, the phase response of the antenna can be determined in addition to the scalar directivity or gain pattern [2].

However, to enable measurements in the frequency ranges above approx. 70 GHz, extension modules are usually needed that multiply the testport signal from moderate frequency ranges (10 GHz to 25 GHz) into the mmWave range. Furthermore, a local oscillator has to be provided and the intermediate frequency signals of the impinging (a) and reflected (b) waves have to be transferred from the integrated reflectometer in each extension module to the receiver architectures within the VNA. Therefore, it is a complex task to mount these modules onto a robotic platform to enable the large degree of mobility needed for antenna measurements. Amongst other reasons, comparably large expensive robotic platforms are needed to carry the weight of the modules (approx. 5 kg). Furthermore, secure cable alignment is of high importance to prevent connector damages and undesired large phase changes due to cable bending.

To overcome these issues, the authors have presented works [3], [4] on robotic antenna measurements enabled by compact frequency-modulated continuous wave (FMCW) radar sensors. These sensors only need a single cable connections for USB or Ethernet control to a remote PC and no RF signals need to be fed or captured. Additionally, they are able to cover large bandwidths of more than 20 GHz [5]. In [4] we presented antenna pattern measurements using a fixed sensor and a corner reflector target for to scan the antenna pattern in W-band. Advancing this concept, we presented [3] an incoherent measurement approach using two FMCW modules using one of those as a spectrum analyzer. In this case, the power loss in the free space transmission is not included with an r^{-4} as in a reflection measurement but only with r^{-2}.

In this contribution, we will present a novel measurement method using a D-band FMCW module [6] in a reflection configuration, similar to [7]. Instead of a passive trihedral target, a horn antenna is used as a probe or reference antenna in conjunction with a switchable load at its feed is introduced to improve the suppression of undesired clutter reflections from the environment and to enhance the dynamic range. By switching between a "Matched Load" and a "Short" at the feed of this reference antenna, a differential measurement is enabled. Thus, all radar and environmental related reflections are strongly suppressed. The most significant benefit is the availability of very fast and high dynamic range broadband measurements. Since the FMCW ramp covers 56 GHz of bandwidth, the broadband antenna pattern is obtained in very short time. Furthermore, the self-coherent FMCW principle provides magnitude and phase-accurate data at a high dynamic range. We will compare this approach previous results and with the state of the art.

In section II, the measurement setup and the signal processing steps are presented and explained in detail. Section III presents measurement results on high-gain lens antennas and compares those to simulations.

II. Measurement Approach

A. Measurement Setup

The measurement setup, depicted in Fig. 1, includes a 6-degree-of-freedom (DOF) compact robot, named HORST 600 from fruitcore robotics, a D-band ultrawideband radar sensor

978-88-31299-10-7/25/$31.00 ©2025 IEEE

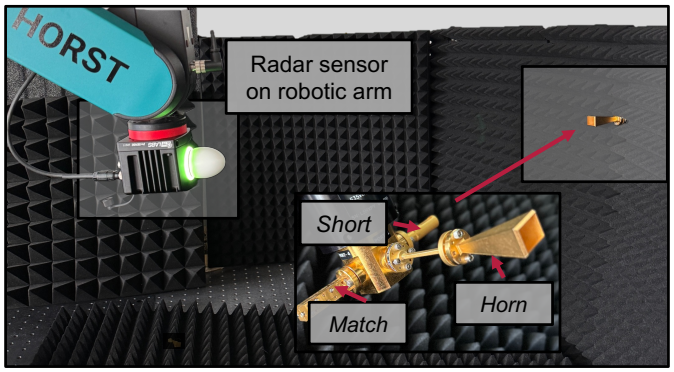

Fig. 1. Photograph of the measurement setup showing the robot and the radar sensor on the left hand side and the reference antenna on the right hand side. A high gain dielectric lens antenna is mounted on the radar sensor. The depicted measurement position corresponds to the main lobe $\varphi = 0$ and $\vartheta = 0$ pointing towards the reference horn antenna.

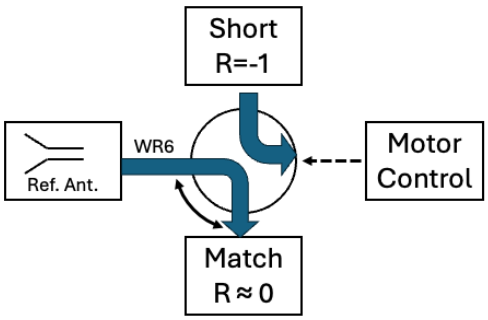

Fig. 2. Block diagram of the reference antenna (20 dBi horn) site including the waveguide switch and the reflection standards.

named X1000 from 2π-Labs [6] as well as a D-band/WR-6 motor controlled electromechanical waveguide switch from miWave. The antenna under test (AUT) is mounted on the radar sensor and is used to radiate and receive the FMCW signal. The radar sensor is mounted on the tool-flange of the robot to enable a pivotal movement around the AUT phase center without the need for large movements. The sensor is connected by an industrial 24 V power cable to the head of the robot. The data and control signals of the sensor are provided via ethernet.

At the fixed reference antenna position in approx 0.5 m distance, the switch connects a 20 dBi WR-6 horn antenna to either a "Matched Load" calibration standard or to a "Short" standard. A block diagram is presented in Fig. 2. Thus the measurement principle is comparable to [7]. By performing two FMCW measurements that only differ by the impedance at the feed of the horn antenna a differential measurement is possible. Therefore, all reflections that are present in both measurements, e.g. sensor reflections, robot reflections, environmental reflections can be removed from the signal.

The setup enables measurements in arbitrary cutting planes of the diagram, e.g. azimuth, elevation or 45° to measure x-pol contributions. Furthermore, spherical scans are possible, as well. The load of the reference antenna is switched after the robot reached each measurement position. In order to further enhance the dynamic range of the measurement, the sensor can easily perform e.g. 1000 measurements at each position, since each FMCW sweep only takes 1 ms and 1 kHz measurement rate can be achieved.

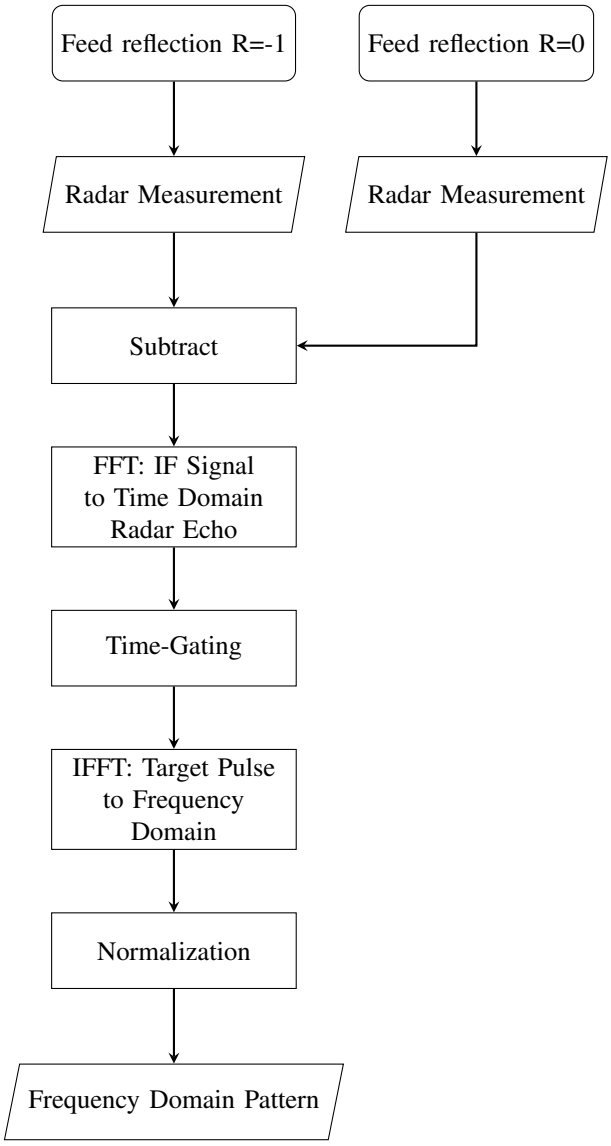

Fig. 3. Flow chart of the signal processing chain.

B. Signal Processing

The signal processing is based on time-gating the complex (magnitude and phase) antenna feed reflection that changes whether the "Short" (R=-1) or "Match" (R≈0) standard are enabled at the motorized switch. In order to obtain the echo profile of the radar sensor, a Fast Fourier Transform (FFT) is applied to the raw intermediate frequency (IF) signal provided by the sensor. A Hamming-Window is used in this transform, since it allows a better window removal after time-gating. This

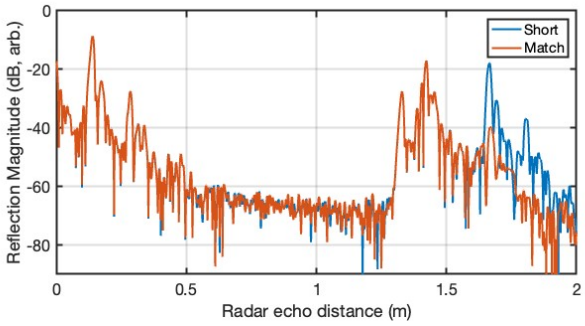

Fig. 4. Radar echoes obtained from the sensor after applying a Hamming-Window. The strong change in the reference antenna's feed impedance can well identified at approx. 1.6 m.

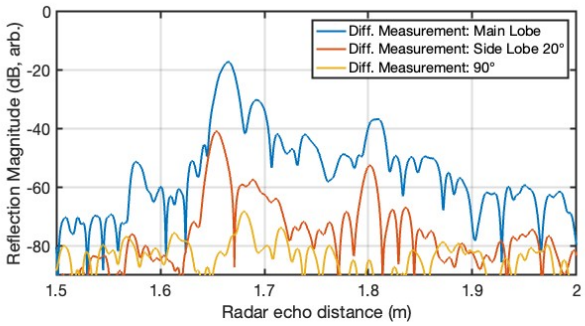

Fig. 5. Differential Radar echoes measured at main lobe, side lobe and under 90°, showing the high dynamic range of approx 60 dB.

is because the Hamming-window function does not approach zero at the first and last bin. A flow-chart of the procedure is shown in Fig. 3.

In addition to evaluating the difference signal between both switch states, a waveguide dispersion compensation is introduced that improves the distorted pulse shape, occurring due to the ultrawideband signal propagating in the hollow waveguides. A waveguide length of 4 cm is assumed here. Figure 4 presents the measured radar echoes at the main lobe position at different switch states. As can be seen from the Figure, the individual measurements contain radar internal and AUT mismatch reflections (up to 0.5 m). At 1.4 m the reference antenna reflection can be seen. The switched load reflection is visible in the "Short" measurement at 1.7 m. Additionally, Fig. 5 presents the differential measurement, where this contribution is most prominent. A dynamic range of more than 60 dB can be identified. Furthermore, Fig. 5 demonstrates that this peak can be well identified even at large angles, i.e. far outside the main lobe. The spherical (i.e. azimuth and elevation scanned) magnitude pattern of the radar echo pulse in time-domain is shown in Fig. 5 for small angles (both, elevation and azimuth are less than 7 degree). It resembles the effective radiation pattern that considers the complete 56 GHz of bandwidth available to the radar sensor.

The broadband signals are afterwards time-gated and re-transformed into the IF domain, which corresponds to the

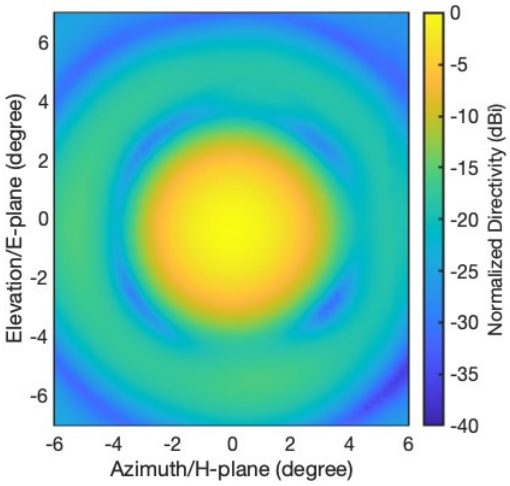

Fig. 6. Effective broadband characteristic of the main lobe, extracted from the radar echo. The echo-pulse response combines the frequency selective radiation pattern into a single pulse, i.e. is the effective pattern applicable to a radar measurement.

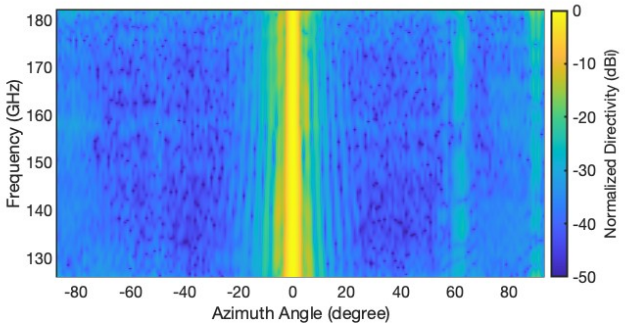

Fig. 7. Broadband antenna pattern measured in azimuth (H-plane) of the test antenna, demonstrating the broadband measurement concept.

transmit frequency domain [8]. Therefore, the desired probe antenna feed reflection is isolated from all other undesired targets and again represented in a frequency resolved domain. In Fig. 7 this broadband directivity measurement is presented. The data is shown along the complete azimuth cutting plane of the hemisphere. In contrast to Fig. 6, the frequency dependent behavior of the AUT can be extracted from this data, e.g. in terms of main lobe width, side lobe levels, and gain.

To cope with the varying output power of the sensor and the changing return loss of the AUT, the pattern is normalized to the value reached within the main lobe for at each frequency point. To determine the varying gain-over-frequency behavior, a two- or three-antenna measurement can be done, as well.

III. Results

In order to evaluate the performance of the measurement setup, a high gain dielectric lens antenna [9] is characterized and compared against the simulation model. The lens is milled from polytetrafluoroethylene (PTFE)/Teflon and provides a nominal directivity of 37.4 dBi at 150 GHz. The lens is of

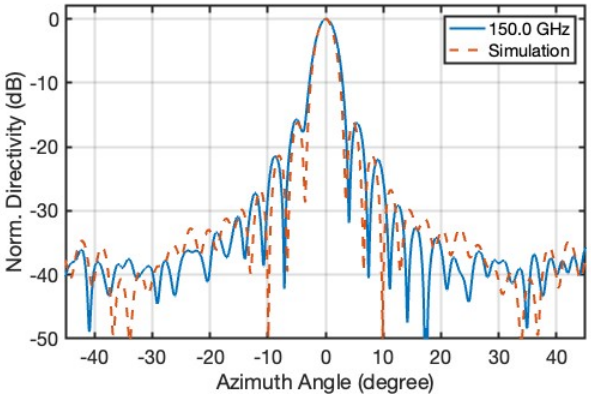

Fig. 8. Measured H-plane antenna pattern of the test antenna at 150 GHz in comparison with the expected behavior simulated with CST Microwave Studio.

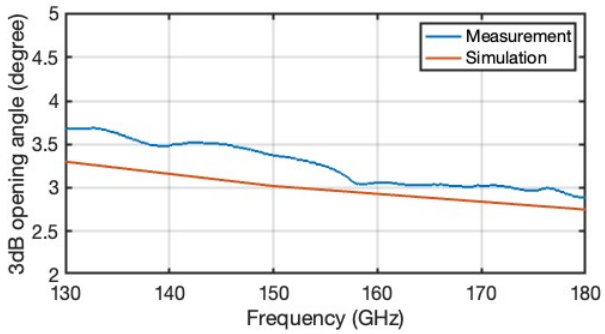

Fig. 9. Broadband evaluation of the 3dB opening angle over frequency in comparison with the simulated characteristic (at 130 GHz, 150 GHz, and 180 GHz).

elliptic shape and fed in one of its internal foci by a quadratic waveguide of 1.6 mm dimensions. It refracts the spherical internal waves to planar waves, thus providing a high gain aperture.

A simulation of the lens and feed structure has been performed in CST Microwave Studio. The copolar directivity plot of the azimuth- (H-)plane 150 GHz is extracted from Fig. 7 and shown as a 1D graph in Fig. 8 to compare the simulated and measured results. The curves agree very well and the measurement nicely exhibits the characteristic far-field zeros in between the sidelobes. The measurement exhibits a high dynamic range of approx. 40 dB in this case. However, from Fig. 8 it appears that the lower measurement limit is not defined by thermal noise but by systematic characteristics that may even correspond to the AUT. From the broadband measurement, the frequency dependent behavior can be extracted. Therefore, the opening angle is extracted as a function of frequency. The result is shown in Fig. 9 and again compared to the expected behavior from simulation. The measurement angle is slightly larger than in the simulation, i.e. by 0.3-0.5 degree. The characteristic narrowing of the main lobe at higher frequencies is well matched.

IV. Conclusion

[10] This paper presented a robotic antenna measurement system that is based on ultrawideband FMCW radar modules. Due to the compactness of the radar module, the AUT on the radar module and easily positioned by a lightweight and cost effective robotic platform. The antenna pattern is measured by performing a differential reflection measurement on a probe antenna providing a switchable load at the probe antenna feed point. This switchable load is realized by a motorized waveguide switch, providing either a ”Short” or a ”Match” calibration standard. Due to the large dynamic range and the ultrawideband measurement provided by the FMCW sensor, coherent antenna pattern measurements covering a complete hemisphere a possible. In addition, a single FMCW measurement is done in milliseconds allowing for comparable fast hemispherical scans while at the same time providing a wideband antenna measurement result.

Acknowledgment

This work was supported in part by the German Research Foundation (DFG) under Project 287022738—TRR 196 and in part by the German Federal Ministry of Education and Research (BMBF) in the course of the 6G research hub under grant number 16KISK038.

References

[1] B. Sievert, J. T. Svejda, D. Erni, and A. Rennings, “Spherical mm-Wave/THz Antenna Measurement System,” *IEEE Access*, vol. 8, pp. 89 680–89 691, 2020.

[2] S. L. Smith, J. W. Archer, G. P. Timms, K. W. Smart, S. J. Barker, S. G. Hay, and C. Granet, “A Millimeter-Wave Antenna Amplitude and Phase Measurement System,” *IEEE Transactions on Antennas and Propagation*, vol. 60, no. 4, pp. 1744–1757, 2012.

[3] K. Dausien, M. Kleinschmidt, I. Rolfes, N. Pohl, and J. Barowski, “Robotic Antenna Characterization System Based on Wideband FMCW Transceiver Modules,” in *2024 18th European Conference on Antennas and Propagation (EuCAP)*, 2024, pp. 1–5.

[4] L. Piotrowsky, V. Bernhardt, J. Barowski, I. Rolfes, and N. Pohl, “Antenna Pattern Characterization With an Industrial Robot Assisted FMCW Radar System,” in *2019 IEEE Asia-Pacific Microwave Conference (APMC)*, 2019, pp. 153–155.

[5] C. Bredendiek, K. Aufinger, and N. Pohl, “Full Octave Continuously Tunable SiGe Bipolar LC-VCO in K u-Band,” in *2021 16th European Microwave Integrated Circuits Conference (EuMIC)*. IEEE, 2022, pp. 277–280.

[6] Kueppers, Simon and Jaeschke, Timo and Pohl, Nils and Barowski, Jan, “Versatile 126–182 GHz UWB D-band FMCW radar for industrial and scientific applications,” *IEEE Sensors Letters*, vol. 6, no. 1, pp. 1–4, 2021.

[7] D. Kruglov, P. Krasov, O. Iupikov, A. Vilenskiy, M. Ivashina, and R. Maaskant, “Contactless measurement of a d-band on-chip antenna using an integrated reflective load switch,” *IEEE Antennas and Wireless Propagation Letters*, 2023.

[8] Barowski, Jan and Zimmermanns, Marc and Rolfes, Ilona, “Millimeter-wave characterization of dielectric materials using calibrated FMCW transceivers,” *IEEE Transactions on Microwave Theory and Techniques*, vol. 66, no. 8, pp. 3683–3689, 2018.

[9] Garten, Orell and Barowski, Jan and Rolfes, Ilona, “Simulation and Optimization of the Design of Focusing Dielectric Lenses based on Cartesian Ovals with Physical Optics,” in *2020 International Workshop on Antenna Technology (iWAT)*. IEEE, 2020, pp. 1–4.

[10] P. Stockel, P. Wallrath, R. Herschel, and N. Pohl, “Detection and Monitoring of People in Collapsed Buildings Using a Rotating Radar on a UAV,” *IEEE Transactions on Radar Systems*, 2023.